XI International Conference on Computational Methods for Coupled Problems in Science and Engineering
COUPLED PROBLEMS 2025
A. Larese, S. Perotto and G. Rozza (Eds)

A FINITE ELEMENT - FINITE VOLUME CODE COUPLING FOR OPTIMAL CONTROL IN BUOYANCY-DRIVEN FLOWS

S. BALDINI*, G. BARBI*, G. BORNIA*, A. CERVONE*, F. GIANGOLINI*, S. MANSERVISI* AND L. SIROTTI*

*Department of Industrial Engineering (DIN)
Alma Mater Studiorum - Università di Bologna
Lab. of Montecuccolino, 40136 Bologna, Italy
e-mail: samuele.baldini2@unibo.it, web page: https://ingegneriaindustriale.unibo.it/it

Key words: Boussinesq approximation, Conjugate Heat Transfer, natural convection, optimal control, code coupling

Abstract. In this work a decoupling approach for solving optimal control problems in buoyancy-driven flows is presented. In detail a finite element code (*FEMuS*) is used for solving the adjoint equations while a finite volume code (*OpenFOAM*) is used for the state equations. In this way, we are able to leverage the variational nature of the finite element method to solve the variational equations arising in the optimality system, while using a validated external code to solve the physical problem, without loss of reliability. The data transfer between the two codes is performed with the external library *MEDCoupling*. Some numerical examples are compared with the non-decoupled finite element solutions in order to validate the proposed approach.

1 INTRODUCTION

One key aspect of designing a engineering system is the analysis of the physical behavior of the variables involved. The numerical solution of partial differential equations describing the physical phenomena provides an effective and advantageous approach for this type of analysis. The simulation process takes as input a set of parameters (such as boundary conditions and material properties) that define the problem, and returns as output the behavior of the system.

However, it is sometimes useful to reverse this process and determine the input data that would lead the physical variables to satisfy certain desired conditions. This approach is known as an inverse problem and can be addressed using various optimization techniques. While a try and fail approach is inaccurate and expensive in terms of both computational and time resources, these numerical optimization methods provide an effective and systematic solution to the inverse problem [4]. The underlying idea is to minimize a cost functional that evaluates the distance between a state variable and its desired target, under the constraints imposed by the physics equations [2].

In this paper, we address the use of the Lagrange multipliers method to formulate the optimal control problem. This approach leads to an optimality system composed of the physical equations (referred to as the state equations), the corresponding adjoint equations, and an optimality condition for the control variables. Both the adjoint system and the optimality conditions are obtained through the variational differentiation of the Lagrangian functional, which combines the

objective functional and the state equations. For this reason, most numerical implementations in this context rely on variational methods, i.e. the Finite Element Method [3].

Nevertheless, in some cases the use of validated, efficient and reliable tools for solving the state equation is essential. While an approach for decoupling the optimal control problem across different codes has already been presented in [10], in this work we aim to extend it to three-dimensional flows. In detail, the state system is solved using the Finite Volume (FV) code OpenFOAM [11], while the adjoint system and the optimality conditions are treated using the Finite Element (FE) code FEMuS [12]. The first one is open-source and widely used in the scientific community, the choice to solve the state equation with it is mainly illustrative. The second one is an in-house code that leverages the variational nature of the Finite Element method to solve the adjoint equation and the optimality condition in their native form.

This work focuses on optimal control problems for natural convection flows. Several studies have addressed such problems and established their mathematical well-posedness, see for instance [5, 6, 7, 8]. Specifically, we address a vorticity minimization inside a three-dimensional differentially heated cavity, either with a volumetric control or a boundary control approach.

The paper is organized as follows: in the first section we introduce the problem and derive the optimality system, in the second one we present the numerical algorithm for the code coupling and finally we provide some numerical tests and compare them with a reference case.

2 OPTIMAL CONTROL PROBLEM

In this section, we introduce the mathematical setting of the optimal control problem. Then, we write the governing equation that describe the physics of natural convection flows. Finally we define the objective functional to minimize and we derive from it the optimality system.

2.1 Mathematical setting

We start presenting some mathematical notation from functional analysis [1]. Considering a generic domain $\Omega \in \mathbb{R}^N$, $H^s(\Omega)$ denotes the standard Sobolev space $W^{s,2}(\Omega)$ of order $s \in \mathbb{R}$, and clearly the space of square-integrable functions $L^2(\Omega)$ refers to the zero-order Sobolev space $H^0(\Omega)$,

$$L^2(\Omega) = \left\{ f \colon \Omega \to \mathbb{R} \;\middle|\; \int_\Omega |f|^2 \, d\Omega < +\infty \right\} .$$

Of particular interest is the space $H^1(\Omega)$ defined as

$$H^1(\Omega) = \left\{ f \in L^2(\Omega) \;\middle|\; \frac{\partial f}{\partial x_k} \in L^2(\Omega), \quad k = 1, 2, \dots, N \right\} ,$$

and we also introduce the subspace of functions that vanish on the boundary $\Gamma \in \partial\Omega$,

$$H^1_\Gamma(\Omega) = \left\{ f \in H^1(\Omega) \mid f = 0 \quad \text{on } \Gamma \right\} .$$

For a generic element f of the Sobolev spaces, its norm in L^2 can be written as

$$||f||_{L^2(\Omega)} = \int_\Omega |f|^2 \, d\Omega \,,$$

while for functions defined only on the boundary of the domain Γ, the norm is defined as

$$||f||_{L^2(\Gamma)} = \int_\Gamma |f|^2 \, d\Gamma \,.$$

Lastly, for $(f, g) \in L^2$ such that $(fg) \in L^1(\Omega)$, where L^1 is the Sobolev space of integrable functions $W^{0,1}$, their inner product is defined as

$$(f, g) = \int_\Omega f\ g\ d\Omega\,.$$

In the case of vector-valued spaces, we indicate them with boldface letters $\mathbf{L}^2, \mathbf{H}^1$. Their norm is defined in a completely analogous manner to the scalar case. Taking $\mathbf{u}, \mathbf{v} \in \mathbf{L}^2(\Omega)$, the inner product is defined as

$$(\mathbf{u}, \mathbf{v}) = \int_\Omega \mathbf{u} \cdot \mathbf{v}\ d\Omega\,.$$

Next, we introduce the bilinear forms

$$\begin{aligned}
a(f, g) &= \int_\Omega \nabla f \cdot \nabla g\ d\Omega && \forall f, g \in H^1(\Omega)\,,\\
a(\mathbf{u}, \mathbf{v}) &= \frac{1}{2}\int_\Omega \left(\nabla \mathbf{u} + \nabla \mathbf{u}^T\right) : \left(\nabla \mathbf{v} + \nabla \mathbf{v}^T\right)\ d\Omega && \forall \mathbf{u}, \mathbf{v} \in \mathbf{H}^1(\Omega)\,,\\
b(\mathbf{u}, f) &= -\int_\Omega f\ \nabla \cdot \mathbf{u}\ d\Omega && \forall \mathbf{u} \in \mathbf{H}^1(\Omega),\ \forall f \in L^2(\Omega)\,,
\end{aligned}$$

and the trilinear forms

$$\begin{aligned}
c(\mathbf{u}, \mathbf{v}, \mathbf{w}) &= \int_\Omega \left((\mathbf{u} \cdot \nabla)\, \mathbf{v}\right) \cdot \mathbf{w}\ d\Omega && \forall \mathbf{u}, \mathbf{v}, \mathbf{w} \in \mathbf{H}^1(\Omega)\,,\\
c(\mathbf{u}, f, g) &= \int_\Omega (\mathbf{u} \cdot \nabla f)\, g\ d\Omega && \forall \mathbf{u} \in \mathbf{H}^1(\Omega),\ \forall f \in H^1(\Omega), \forall g\ \in L^2(\Omega)\,,
\end{aligned}$$

that will be useful in the description of the optimality systems.

2.2 Boussinesq problem

In this section we derive the optimality system for the Boussinesq problem in a cube domain Ω. In this approximation, the physical properties are assumed to be constant with respect to temperature variations, except for the density, which varies only in the gravity term. The Boussinesq approximation is valid only for small temperature variations and is used to model natural convection flows, where buoyancy forces arise from temperature-induced density variations in the gravitational term.

The flow is described from the steady Navier-Stokes equation with a wall condition on the boundary

$$\begin{cases}
\nabla \cdot \mathbf{u} = 0 & \text{on } \Omega\,,\\
-2\nu \nabla \cdot \mathcal{D}(\mathbf{u}) + (\mathbf{u} \cdot \nabla)\mathbf{u} = -\nabla p + \beta \mathbf{g}(T - T_{\text{ref}}) & \text{on } \Omega\,,\\
\mathbf{u} = 0 & \text{on } \partial\Omega\,,
\end{cases} \tag{1}$$

where $\mathbf{u}$ is the velocity field, p is the pressure field, ν is the kinematic viscosity, β is the thermal expansion coefficient, $\mathbf{g}$ is a vector representing the gravitational acceleration in the negative z direction, and $\mathcal{D}(\mathbf{u}) = \frac{1}{2}(\nabla \mathbf{u} + \nabla \mathbf{u}^T)$ is the rate of deformation tensor of the flow.

The temperature distribution inside the cavity is modeled through the steady heat equation

$$\begin{cases} -\alpha \Delta T + \mathbf{u} \cdot \nabla T = Q & \text{on } \Omega\,, \\ T = g_D & \text{on } \Gamma_D \\ \frac{\partial T}{\partial n} = g_N & \text{on } \Gamma_N\,, \end{cases} \tag{2}$$

where T is the temperature field, Q is a generic volumetric heat source, g_N is a generic wall heat flux, g_D is a given temperature profile at the boundary and α is the thermal diffusivity coefficient. The temperature gradient inside the cavity is generated fixing different Dirichlet conditions on opposite walls. The parameters Q and g_N will act as control variables for the vorticity minimization.

The state constraints (1) and (2) are finally written in their weak form using the defined linear, bilinear and trilinear forms

$$\begin{cases} b(\mathbf{u}, f) = 0 & \forall\, f \in L^2(\Omega)\,, \\ \nu a(\mathbf{u}, \boldsymbol{\psi}) + c(\mathbf{u}, \mathbf{u}, \boldsymbol{\psi}) = -b(\boldsymbol{\psi}, p) + (\beta \mathbf{g}(T - T_{ref}), \boldsymbol{\psi}) & \forall\, \boldsymbol{\psi} \in \mathbf{H}^1_{\partial\Omega}(\Omega)\,, \\ \alpha a(T, \phi) + c(\mathbf{u}, T, \phi) = (Q, \phi) + (g_N, \phi)_{\Gamma_N} & \forall\, \phi \in H^1_{\Gamma_D}(\Omega)\,. \end{cases} \tag{3}$$

We define the objective functional for the vorticity minimization as

$$\mathcal{F}(\mathbf{u}, Q, g_N) = \frac{1}{2} \int_\Omega |\nabla \times \mathbf{u}|^2 \, d\Omega + \frac{\lambda_Q}{2} \int_\Omega |Q|^2 \, d\Omega + \frac{\lambda_N}{2} \int_{\Gamma_N} |g_N|^2 \, d\Gamma\,, \tag{4}$$

where λ_Q, λ_N are regularization coefficients for the corresponding control variables. Next, we introduce the Lagrange multipliers $(\boldsymbol{\xi}, \mu, \theta)$, namely the adjoint variables, and we write the Lagrange equation

$$\begin{aligned} \mathcal{L}(\mathbf{u}, p, T, \boldsymbol{\xi}, \mu, \theta) =& \frac{1}{2}(\nabla \times \mathbf{u}, \nabla \times \mathbf{u})_\Omega + \frac{\lambda_Q}{2}(Q, Q)_\Omega + \frac{\lambda_N}{2}(g_N, g_N)_{\Gamma_N} + \\ & - b(\mathbf{u}, \mu) + \\ & + \nu a(\mathbf{u}, \boldsymbol{\xi}) + c(\mathbf{u}, \mathbf{u}, \boldsymbol{\xi}) + b(\boldsymbol{\xi}, p) - (\beta \mathbf{g}(T - T_{ref}), \boldsymbol{\xi}) + \\ & + \alpha a(T, \theta) + c(\mathbf{u}, T, \theta) - (Q, \theta) - (g_N, \theta)_{\Gamma_N}\,. \end{aligned} \tag{5}$$

Differentiating the Lagrangian in the state directions we derive the adjoint system, that reads

$$\begin{cases} b(\boldsymbol{\xi}, \widetilde{p}) = 0 & \forall\, \widetilde{p} \in L^2(\Omega)\,, \\ \nu a(\widetilde{\mathbf{u}}, \boldsymbol{\xi}) + c(\widetilde{\mathbf{u}}, \mathbf{u}, \boldsymbol{\xi}) + c(\mathbf{u}, \widetilde{\mathbf{u}}, \boldsymbol{\xi}) - b(\widetilde{\mathbf{u}}, \mu) = (\nabla \times \boldsymbol{u}, \nabla \times \widetilde{\mathbf{u}}) - c(\widetilde{\mathbf{u}}, T, \theta) & \forall\, \widetilde{\mathbf{u}} \in \mathbf{H}^1_{\partial\Omega}(\Omega)\,, \\ \alpha a(\widetilde{T}, \theta) + c(\mathbf{u}, \widetilde{T}, \theta) = (\beta \mathbf{g} \widetilde{T}, \boldsymbol{\xi}) & \forall\, \widetilde{T} \in H^1_{\Gamma_D}(\Omega)\,, \end{cases} \tag{6}$$

and doing the same process for the control variables we obtain the optimality conditions

$$\begin{aligned} \lambda_Q(Q, \widetilde{Q}) = (\theta, \widetilde{Q}) \qquad & \forall\, \widetilde{Q} \in L^2(\Omega)\,, \\ \lambda_N(g_N, \widetilde{g_N})_{\Gamma_N} = (\theta, \widetilde{g_N})_{\Gamma_N} \quad & \forall\, \widetilde{g_N} \in L^2(\Gamma_N)\,. \end{aligned} \tag{7}$$

From the latter equations we can find the functional derivatives in the control directions, that are needed for the control update

$$\begin{aligned} \frac{\partial \mathcal{L}}{\partial Q} &= \theta + \lambda_Q Q\,, \\ \frac{\partial \mathcal{L}}{\partial g_N} &= \theta + \lambda_N g_N\,. \end{aligned} \tag{8}$$

As we observe, the adjoint equations and optimality conditions naturally appear in an integrable form. Therefore, the most natural approach is to solve them using the finite element method, as we do in this paper.

2.3 Minimization method

The optimality system consists of the state, adjoint, and control equations, which are mutually coupled but solved separately. While the state and adjoint systems are handled using a fixed-point iteration method, convergence of the control variable is ensured through a basic steepest descent algorithm. This method is demonstrated to converge for a sufficiently small step-size. The control update is done with a gradient method, firstly taking the variation δq of the control as

$$\delta Q = -\rho(\theta + \lambda_Q Q)\,,$$
$$\delta g_N = -\rho(\theta + \lambda_N g_N)\,,$$

and then performing the update

$$q_{k+1} = q_k + \delta q\,.$$

3 COMPUTATIONAL FRAMEWORK

In this section, we present the general numerical setup. We first illustrate the coupling algorithm that manages the data transfer between the two codes, and then briefly describe the numerical discretization of each code.

3.1 Coupling algorithm

The reason for choosing a finite element solver for the adjoint and control systems has been discussed in detail in the previous sections. Coupling these with an external solver for the state equation allows for a decoupled approach, giving us the flexibility to select the most suitable solver for our purposes. Specifically we use the in-house code *FEMuS* for the finite element part, while the state system is handled with the finite volume code *OpenFOAM*.

The data exchange is handled using the external library *MEDCoupling*, which is a module of the *MED* library and part of the *Salome* platform. For each code, specific wrappers are created to translate internal data structures into the *MED* format. The interpolation between the different codes is then performed using *MED* routines applied to the corresponding *MED* surrogates. This hub-and-spoke structure facilitates data transfer in the case of a large number of involved codes. In fact, each of them only requires the development of an interface (a wrapper to MED), without the need to connect each code to every other one. A more detailed description of the coupling approach can be found in [9].

The interpolation from *OpenFOAM* to *FEMuS* involves the transfer of the state variables $\mathbf{u}$ and T volumetric fields. Instead the one from *FEMuS* to *OpenFOAM* involves the exchange of the control field, that can be either volumetric in case of the distributed approach Q or only at the boundary in case of the Neumann control g_N. If the the data transfer is volumetric the *MED* surrogate's mesh represents all the simulation domain and three-dimensional interpolation routines are used. On the other hand, if the exchange is performed only at the boundary, only the boundary patch is created in the *MED* format, and two-dimensional interpolation is performed.

3.2 Numerical discretization

The above mentioned interpolation between the different computational grids of the the two codes also involves the projection of the fields from the discrete space of the source code to the one of the target. We introduce the finite dimensional spaces $X_h \subset X = H^1_{\Gamma_D}(\Omega)$, $Q_h \subset L^2(\Omega)$ and $S_h \subset L^2(\Omega)$. Given a domain partition $\mathcal{T}_h$ with the generic element K, and the space of polynomials $\mathcal{P}^r$ of degree at most r they reads

$$
\begin{aligned}
X_h &= \{v_h \in C^0(\bar{\Omega}) : \, v_h|_K \in \mathcal{P}_2 \quad \forall K \in \mathcal{T}_h\}\,, \\
Q_h &= \{v_h \in C^0(\bar{\Omega}) : \, v_h|_K \in \mathcal{P}_1 \quad \forall K \in \mathcal{T}_h\}\,, \\
S_h &= \{v_h \in L^2(\Omega) : \, v_h|_K \in \mathcal{P}_0 \quad \forall K \in \mathcal{T}_h\}\,,
\end{aligned}
$$

and we refer to the vector-valued spaces with bold symbols.

Regarding the discrete state variables which belong to the finite volume discretization, we consider a piece-wise costant approximation, i.e. $\mathbf{u}_h \in \mathbf{S}_h$ and $p_h, T_h \in S_h$. We point out that *OpenFOAM* solves the Navier-Stokes equation with a projection method, specifically we used the PIMPLE algorithm. Passing to the finite element system, the adjoint Navier-Stokes variables $\boldsymbol{\xi}$ and μ are solved in a monolithic way and discretized with the standard Taylor-Hood pair, i.e. $(\boldsymbol{\xi}_h, \mu_h) \in \mathbf{X}_h \times Q_h$. Lastly the adjoint temperature and the controls are addressed with biquadratic finite elements, thus we have $\theta_h, q_h \in X_h$.

4 NUMERICAL RESULTS

In this section, two numerical example are reported to show the effectiveness of the presented methodology. The first test address the vorticity minimization with a distributed control approach, while the other two solve the same minimization problem but with a Neumann boundary control with one controlled boundary. The Neumann control shares the same mathematical formulation as the distributed control, with the difference that it is defined only on the boundary of the domain. In this way, we can assume the interpolation error to be the same when solving the adjoint system, allowing for a clearer analysis of the error when exchanging the volumetric or boundary source.

Each test was carried out using both a coarse and a fine grid. Specifically, for the finite element grid, a $10 \times 10 \times 10$ element biquadratic mesh was used for the coarse case, and a $20 \times 20 \times 20$ mesh for the fine case. For the finite volume code, we employed grids that are approximately equivalent in terms of degrees of freedom, namely $20 \times 20 \times 20$ for the coarse case and $40 \times 40 \times 40$ for the fine case.

The domain of the simulation

$$
\Omega = \{(x, y, z) \in \mathbb{R}^3 : x \in [0, 1], y =\in [0, 1], z =\in [0, 1]\}\,,
$$

is shown in Figure 1, where $\Gamma_D \cup \Gamma_N = \partial\Omega$ and $\Gamma_D \cap \Gamma_N = \emptyset$. As illustrated in the first section we treat Γ_D as a Dirichlet type boundary and Γ_N as a Neumann one. Moreover, we define the following subspaces

$$
\Gamma_l = \{(x, y, z) \in \mathbb{R}^3 \cap \Gamma_D : x = 0, y =\in [0, 1], z =\in [0, 1]\},
$$

and

$$
\Gamma_r = \{(x, y, z) \in \mathbb{R}^3 \cap \Gamma_D : x = 1, y =\in [0, 1], z =\in [0, 1]\}\,,
$$

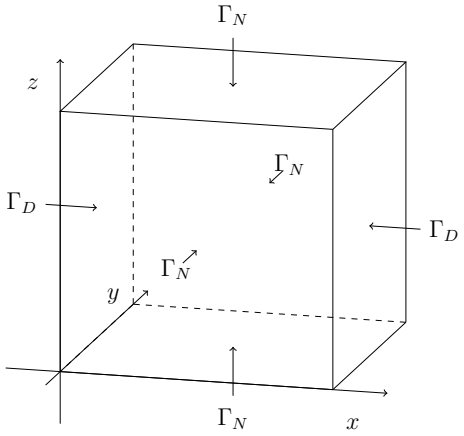

Figure 1: Domain of the Boussinesq problem.

where two different fixed temperature conditions will be imposed on, which will act as source for the buoyancy force. The natural convection intensity strongly depends on the physical properties of the system, and for the presented results we used a Rayleigh number calculated as

$$\mathrm{Ra} = \frac{|\mathbf{g}|\,\beta\,(T_h - T_c)\,L^3}{\nu\,\alpha} \approx 10^3\,,$$

where $|\mathbf{g}| = 9.81$, $\beta = 1$, $\nu = 10^{-2}$, $\alpha = 1$, $L = 1$, the hot temperature $T_h = 1$ and the cold one $T_c = 0$.

4.1 Distributed control

For the distributed control we set $\lambda_N = 0$ and $\lambda_Q = 1 \times 10^{-1}$, and in Table 1 we show the imposed boundary conditions.

Table 1: Boundary conditions for the distributed control problem for each unknown $(\mathbf{u}, T, \boldsymbol{\xi}, \theta)$ on each portion of the boundary

	Γ_l	Γ_r	Γ_N
$\mathbf{u}$	$\mathbf{u} = 0$	$\mathbf{u} = 0$	$\mathbf{u} = 0$
T	$T = T_h$	$T = T_c$	$\nabla T \cdot \mathbf{n} = 0$
$\boldsymbol{\xi}$	$\boldsymbol{\xi} = 0$	$\boldsymbol{\xi} = 0$	$\boldsymbol{\xi} = 0$
θ	$\theta = 0$	$\theta = 0$	$\nabla \theta \cdot \mathbf{n} = 0$

In Figure 2 we provide a comprehensive view on the overall system behavior by plotting all the variables on the domain's symmetry plane. The control acts near the boundary with fixed temperature, heating the region near the cold wall and cooling the region near the hot one. This mechanism creates a nearly isothermal central zone, thereby reducing the buoyancy forces. As a result, two smaller vortices form near the side walls. Clearly, the control is equal to the negative adjoint temperature, scaled by the inverse of λ_N.

We now compare the coupled results with the solution obtained using only the finite element method. Specifically, in Figures 3 and 4, we present a comparison between the state velocity

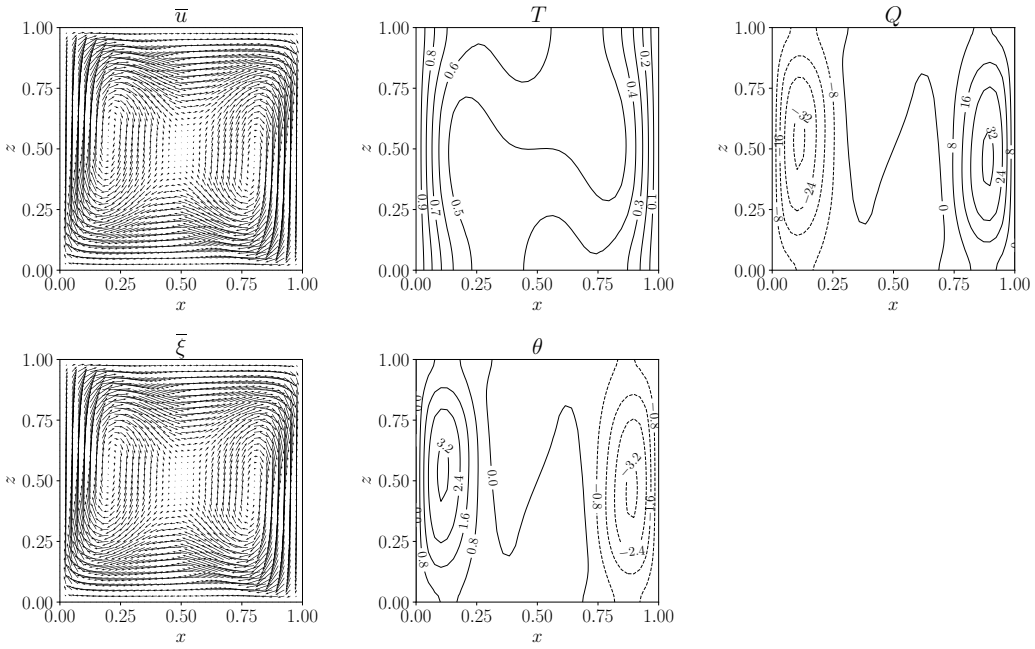

Figure 2: From top-left to bottom-right: glyph of $\mathbf{u}$, contour of T, contour of Q, glyph of $\boldsymbol{\xi}$ and contour of θ, on the plane $\{(x, y, z) \in \mathbb{R}^3 : x \in [0, 1], y = 0.5, z \in [0, 1]\}$.

field $\mathbf{u}$ and the control variable Q, for the coarse and the fine case respectively. We notice a good agreement in the results.

For a more detailed analysis we also report the numerical discrepancies between the solution and on the global functional in Table 2. We refer to the distance between the coupled and the finite element solution as the *error*, since the finite element solution serves as the reference case in this paper. In all cases, the distance between the two approaches is small. However, we observe that this difference decreases with the grid refinement, as interpolation errors become less significant.

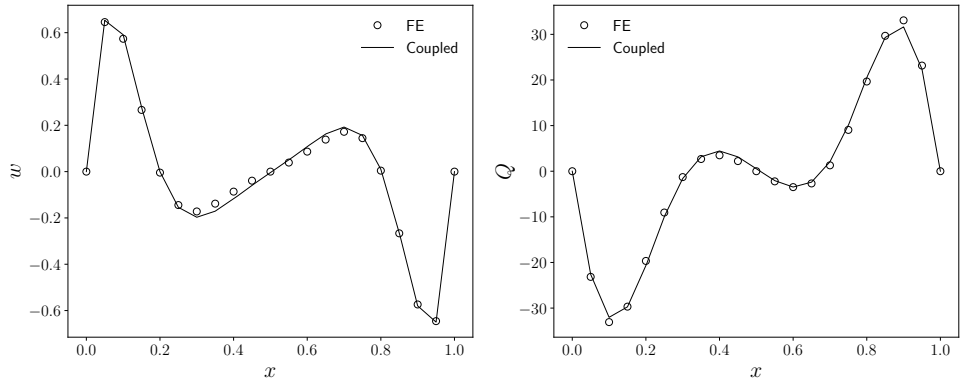

Figure 3: Comparison of the coarse coupled and only FE solutions for $w = \mathbf{u}_z$ (left) and Q (right), along the line $\{(x, y, z) \in \mathbb{R}^3 : x \in [0, 1], y = 0.5, z = 0.5\}$.

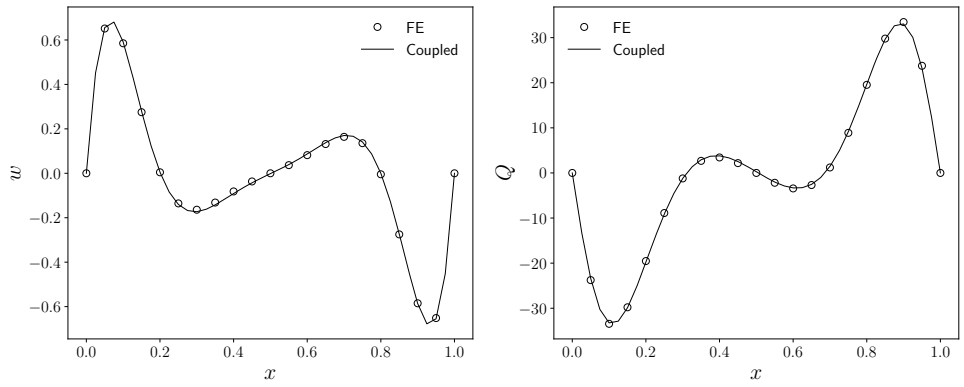

Figure 4: Comparison of the fine coupled and only FE solutions for $w = \mathbf{u}_z$ (left) and Q (right), along the line $\{(x, y, z) \in \mathbb{R}^3 : x \in [0, 1], y = 0.5, z = 0.5\}$.

Table 2: Comparison of the vorticity norm, the control norm, and the value of the cost functional for coarse and fine meshes.

	Coarse			Fine		
	$\|\|\nabla \times \mathbf{u}\|\|^2_{L^2(\Omega)}$	$\|\|Q\|\|^2_{L^2(\Omega)}$	$\mathcal{F}(\mathbf{u}, Q)$	$\|\|\nabla \times \mathbf{u}\|\|^2_{L^2(\Omega)}$	$\|\|Q\|\|^2_{L^2(\Omega)}$	$\mathcal{F}(\mathbf{u}, Q)$
Uncontrolled	1.48×10^2	0	7.4×10^1	1.54×10^2	0	7.7×10^1
Coupled	1.39×10^1	1.58×10^2	1.49×10^1	1.80×10^1	1.61×10^2	1.71×10^1
FE	1.35×10^1	1.61×10^2	1.48×10^1	1.79×10^1	1.62×10^2	1.70×10^1
Error	2.88%	1.86%	0.67%	0.56%	0.62%	0.58%

4.2 Neumann boundary control

For the Neumann boundary control we set $\lambda_Q = 0$ and $\lambda_N = 1 \times 10^{-1}$. We also introduce the controlled boundary

$$\Gamma_c = \{(x, y, z) \in \mathbb{R}^3 \cap \Gamma_N : x =\in [0, 1], y =\in [0, 1], z = 0\},$$

where the control g_N is applied. The imposed boundary conditions are summarized in Table 3.

Table 3: Boundary conditions for the distributed control problem for each unknown $(\mathbf{u}, T, \boldsymbol{\xi}, \theta)$ on each portion of the boundary

	Γ_l	Γ_r	Γ_c	Γ_N
$\mathbf{u}$	$\mathbf{u} = 0$	$\mathbf{u} = 0$	$\mathbf{u} = 0$	$\mathbf{u} = 0$
T	$T = T_h$	$T = T_c$	$\nabla T \cdot \mathbf{n} = g_N$	$\nabla T \cdot \mathbf{n} = 0$
$\boldsymbol{\xi}$	$\boldsymbol{\xi} = 0$	$\boldsymbol{\xi} = 0$	$\boldsymbol{\xi} = 0$	$\boldsymbol{\xi} = 0$
θ	$\theta = 0$	$\theta = 0$	$\nabla \theta \cdot \mathbf{n} = 0$	$\nabla \theta \cdot \mathbf{n} = 0$

As in the previous case, in Figure 5 we plot all the volumetric variables of the optimality system on the symmetry plane of the domain. We can observe that the influence of the control is limited to the bottom part of the domain, where it is applied. Indeed, the flow in the upper

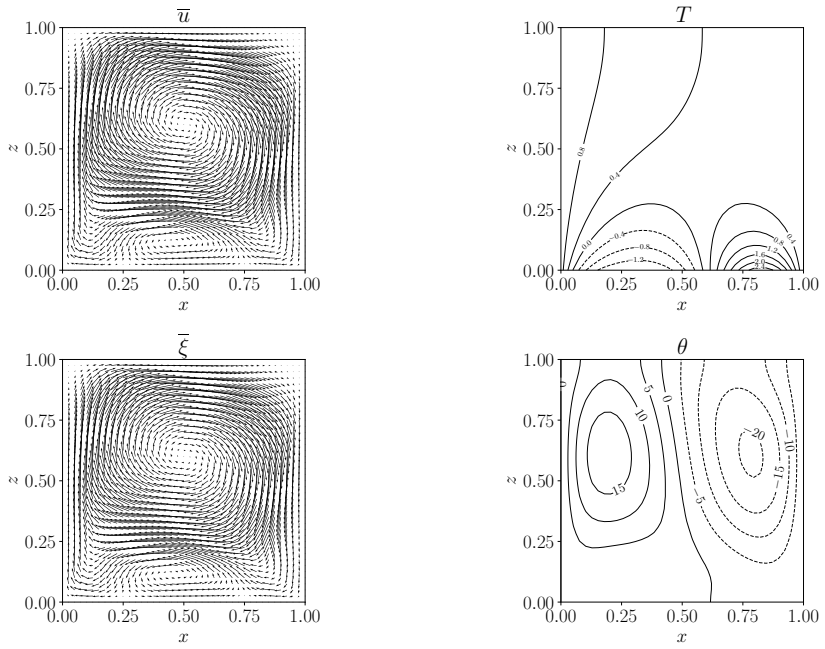

Figure 5: From top-left to bottom-right: glyph of $\mathbf{u}$, contour of T, glyph of $\boldsymbol{\xi}$ and contour of θ, on the plane $\{(x, y, z) \in \mathbb{R}^3 : x \in [0, 1], y = 0.5, z \in [0, 1]\}$.

region is approximately invariant. In fact, by looking at the adjoint temperature plot, we observe that it is mostly concentrated in the upper part of the domain.

Finally, we show the comparison of the coupled and the only finite element approaches, in Figure 6 for the coarse case and in Figure 7 for the fine one. Generally, a good agreement is found. Again, we show the numerical errors in Table 4. We observe overall higher errors compared to the distributed control case, especially in the objective functional term, which involves the state velocity $\mathbf{u}$ solved using the finite volume framework. However, the discrepancies decrease as the grid is refined, consistently with the previous case.

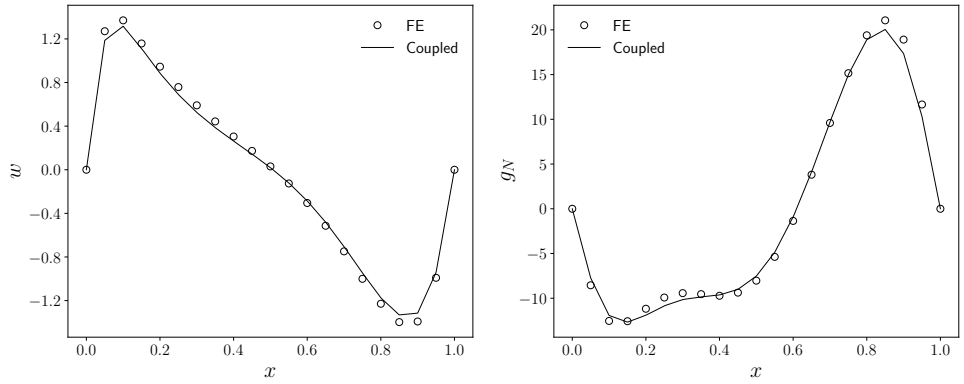

Figure 6: Comparison of the coarse coupled and only FE solutions for $w = \mathbf{u}_z$ (left) along the line $\{(x, y, z) \in \mathbb{R}^3 : x \in [0, 1], y = 0.5, z = 0.5\}$, and g_N (right) along the line $\{(x, y, z) \in \mathbb{R}^3 : x \in [0, 1], y = 0.5, z = 0\}$.

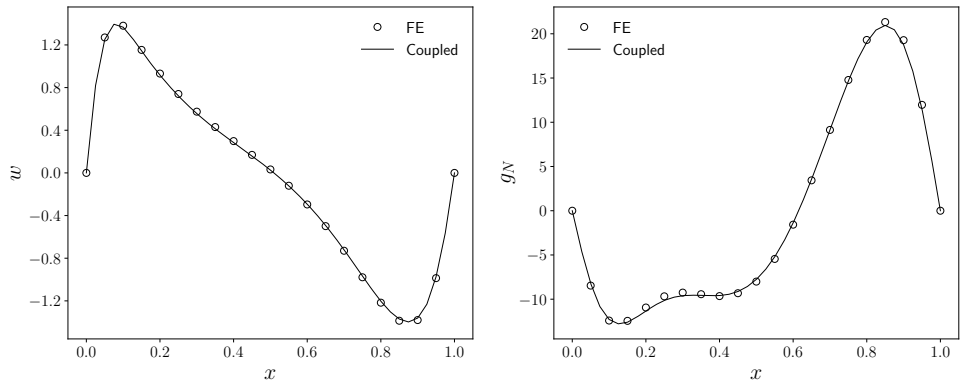

Figure 7: Comparison of the fine coupled and only FE solutions for $w = \mathbf{u}_z$ (left) along the line $\{(x, y, z) \in \mathbb{R}^3 : x \in [0, 1], y = 0.5, z = 0.5\}$, and g_N (right) along the line $\{(x, y, z) \in \mathbb{R}^3 : x \in [0, 1], y = 0.5, z = 0\}$.

Table 4: Comparison of the vorticity norm, the control norm, and the value of the cost functional for coarse and fine meshes.

	Coarse			Fine		
	$\|\|\nabla \times \mathbf{u}\|\|^2_{L^2(\Omega)}$	$\|\|g_N\|\|^2_{L^2(\Gamma_c)}$	$\mathcal{F}(\mathbf{u}, g_N)$	$\|\|\nabla \times \mathbf{u}\|\|^2_{L^2(\Omega)}$	$\|\|g_N\|\|^2_{L^2(\Gamma_c)}$	$\mathcal{F}(\mathbf{u}, g_N)$
Uncontrolled	1.48×10^2	0	7.4×10^1	1.54×10^2	0	7.7×10^1
Coupled	6.82×10^1	1.14×10^2	3.98×10^1	8.75×10^1	1.17×10^2	4.96×10^1
FE	7.58×10^1	1.17×10^2	4.38×10^1	9.03×10^1	1.18×10^2	5.11×10^1
Error	10.0%	2.56%	9.13%	3.10%	0.85%	2.94%

5 Conclusions

This paper presents a code coupling strategy to decouple the optimality system in optimal control problems, employing a finite element code for the adjoint and control variables and an external solver for the physical ones. Specifically, the approach proposed in [9] is extended to the optimization of three-dimensional natural convection flows. We focus on a vorticity minimization problem in a cube cavity and explore both distributed and Neumann boundary control strategies. In both cases, the results show good agreement with the reference solution, although the boundary control exhibits slightly higher errors. Nonetheless, for both control strategies, the discrepancies decrease as the grid is refined.

Future researches will implement a more in-depth analysis of the above mentioned errors and apply this approach to real world applications, where the use of an external solver for the state equation is more clearly justified.

REFERENCES

[1] Adams, Robert A and Fournier, John JF *Sobolev spaces*. Springer (2003).

[2] Manzoni, Andrea and Quarteroni, Alfio and Salsa, Sandro *Optimal control of partial differential equations*. Springer (2021).

[3] Vivette, Girault and Pierre-Arnaud , Raviart *Finite Element Methods for Navier-Stokes Equations*. Springer (2012).

[4] Gunzburger, Max D *Perspectives in flow control and optimization*. SIAM (2002).

[5] Lee, Hyung-Chun and Imanuvilov, O Yu *Analysis of Neumann boundary optimal control problems for the stationary Boussinesq equations including solid media*. SIAM Journal on Control and Optimization (2000).

[6] Lee, Hyung-Chun and Imanuvilov, O Yu *Analysis of optimal control problems for the 2-D stationary Boussinesq equations*. Journal of mathematical analysis and applications (2000).

[7] Li, Shugang *Optimal controls of Boussinesq equations with state constraints*. Journal of mathematical analysis and applications (2005).

[8] Fursikov, Andrei V and Imanuvilov, O Yu *Local exact boundary controllability of the Boussinesq equation*. SIAM Journal on Control and optimization (1998).

[9] Barbi, Giacomo and Cervone, Antonio and Giangolini, Federico and Manservisi, Sandro and Sirotti, Lucia *Numerical Coupling between a FEM Code and the FVM Code OpenFOAM Using the MED Library*. Applied Sciences (2024).

[10] Baldini, Samuele and Barbi, Giacomo and Cervone, Antonio and Giangolini, Federico and Manservisi, Sandro and Sirotti, Lucia *Optimal Control of Heat Equation by Coupling FVM and FEM Codes*. Mathematics (2025).

[11] Jasak, Hrvoje and Jemcov, Aleksandar and Tukovic, Zeljko and others *OpenFOAM: A C++ library for complex physics simulations*. International workshop on coupled methods in numerical dynamics (2007).

[12] Barbi, Giacomo and Bornia, Giorgio and Cerroni, Daniele and Cervone, Antonio and Chierici, Andrea and Chirco, Leonardo and Viá, Roberto and Giovacchini, Valentina and Manservisi, Sandro and Scardovelli, Ruben and others *FEMuS-Platform: A numerical platform for multiscale and multiphysics code coupling*. 9th International Conference on Computational Methods for Coupled Problems in Science and Engineering, COUPLED PROBLEMS 2021 (2021).